PHYSICAL REVIEW D **96,** 124001 (2017)

Charged scalar perturbations on charged black holes in de Rham-Gabadadze-Tolley massive gravity

Piyabut Burikham[*]

High Energy Physics Theory Group, Department of Physics, Faculty of Science, Chulalongkorn University, Phyathai Road, Bangkok 10330, Thailand

Supakchai Ponglertsakul[†]

Theoretical and Computational Physics Group, Theoretical and Computational Science Center (TaCS), Faculty of Science, King Mongkut's University of Technology Thonburi, Prachautid Road, Bangkok 10140, Thailand

Lunchakorn Tannukij[‡]

Department of Physics, Faculty of Science, Mahidol University, Bangkok 10400, Thailand and Department of Physics, Hanyang University, Seoul 133-891, South Korea

(Received 19 September 2017; published 1 December 2017)

We explore the quasistationary profile of a massive charged scalar field in a class of charged black holes in de Rham-Gabadadze-Tolley (dRGT) massive gravity. We discuss how the linear term in the metric, which is a unique character of the dRGT massive gravity, affects the structure of the spacetime. Numerical calculations of the quasinormal modes are performed for a charged scalar field in the dRGT black hole background. For an asymptotically de Sitter (dS) black hole, an improved asymptotic iteration method is used to obtain the associated quasinormal frequencies. The unstable modes are found for the $\ell = 0$ case, and their corresponding real parts satisfy the superradiant condition. For $\ell = 2$, the results show that all the de Sitter black holes considered here are stable against a small perturbation. For an asymptotically dRGT anti-de Sitter (AdS) black hole, unstable modes are found with the frequency satisfying the superradiant condition. Effects of massive-gravity parameters are discussed. Analytic calculation reveals the unique diffusive nature of quasinormal modes in the massive-gravity model with the linear term. Numerical results confirm the existence of the characteristic diffusive modes in both the dS and AdS cases.

DOI: 10.1103/PhysRevD.96.124001

I. INTRODUCTION

Massive gravity is a modified gravity theory in which gravity is described by a massive spin-2 graviton, propagating 5 degrees of freedom. Unlike general relativity in which the graviton is massless, the gravitation in massive gravity is essentially modified at the scale corresponding to the graviton mass m_g. In cosmological aspects, we might expect this characteristic to be responsible for the cosmic accelerating expansion given that the graviton mass is of the same order as the Hubble parameter; $m_g \sim H \sim 10^{-33}$ eV [1]. On the other hand, the recent observation from the Laser Interferometer Gravitational-Wave Observatory (LIGO) on a binary black hole merger, GW150914, has put an upper bound, $m_g \leq 1.2 \times 10^{-22}$ eV, on the graviton mass [2] (see also Ref. [3] for graviton mass bounds from other aspects). From a cosmological point of view, massive gravity is still a viable model of the Universe.

The very first model of massive gravity was realized as a linear theory by Fierz and Pauli (FP) in 1939 [4]. The FP massive gravity suffers from the van Dam-Veltman-Zakharov (vDVZ) discontinuity in which the predictions made by the FP theory do not coincide with those made by general relativity when an appropriate limit (massless-graviton limit) is taken [5,6]. After that, Vainshtein suggested that because of the introduction of the graviton mass the graviton mass introduces a new scale known as the Vainshtein radius, outside which the FP theory works with good accuracy [7]. For the massless limit, however, this scale is pushed toward infinity so that the linear theory cannot be trusted when being used for local systems, and nonlinear effects should be included in order to cure the vDVZ discontinuity [7]. (See, however, Ref. [8], in which the vDVZ discontinuity can be evaded). It was found by Boulware and Deser that generic nonlinear massive-gravity theories always propagate 6 degrees of freedom instead of 5 and the additional degree of freedom unfortunately has wrong-sign kinetic energy [known as a Boulware-Deser (BD) ghost], causing an instability in the theories [9]. In 2010, de Rham, Gabadadze, and Tolley found that there exists a class of nonlinear massive-gravity theory that does

[*]piyabut@gmail.com
[†]supakchai.p@gmail.com
[‡]l_tannukij@hotmail.com

not possess the BD ghost, dubbed dRGT massive gravity [10,11]. Since this theory is constructed successfully without the well-known pathology, it actually gives rise to various kinds of studies in massive gravity such as cosmological solutions [12,13], cosmological perturbations [14], black hole solutions and thermodynamics [15,16], and even various generalizations of the dRGT theory, like the quasidilaton theory [17,18]. Recently, a black hole solution to dRGT massive gravity has been found [15,16], and the solution is in agreement with the dRGT cosmology in that the graviton mass effectively plays the role of cosmological constant. It was also found that the solution can be stable in the thermodynamics language [15,16].

A bosonic field can be used to extract rotational energy and electric charge from a black hole via the so-called superradiant scattering. The amplitude of the bosonic field will be amplified if its frequency satisfies the following condition (for asymptotically flat spacetime) [19]

$$\omega < m\Omega_H + q\Phi_H. \tag{1}$$

In the above condition, m is the azimuthal number; q is the particle charge; and Ω_H and Φ_H are the angular velocity and electrostatic potential at the black hole horizon, respectively. The superradiant phenomena can often lead to an instability of the spacetime background if the superradiant mode is confined near the black hole horizon. The amplitude of the bosonic field will be amplified repeatedly, causing a non-negligible backreaction on the exterior geometry.

In standard general relativity, the complex scalar field on the Reissner-Nordström (RN) background is known to suffer from superradiant instability. For example, the massive charged scalar field on RN enclosed with a mirrorlike boundary condition experiences charged superradiant instability [20]. Time domain analysis [21] on this system reveals that the unstable modes grow a lot faster than in the rotating case. Moreover, a massless charged scalar field on a small RN black hole in asymptotically anti-de Sitter (AdS) spacetime is shown to be superradiantly unstable [22]. Despite RN in asymptotically flat spacetime being stable against spherically symmetric charged scalar perturbations, however, an instability of the RN black hole in asymptotically de Sitter spacetime has been surprisingly discovered [23]. It is shown in Ref. [24] that instability occurs when the scalar field's frequency satisfies the superradiant condition. It should be noted that not all the superradiant modes are unstable; the instability holds only for the spherical perturbation $\ell = 0$ mode, while the superradiant mode exists in higher ℓ.

For the rotating case, superradiant instability of the massless scalar field on the Kerr background enclosed with a reflecting mirror is found [25]. For nonasymptotically flat spacetime, a scalar perturbation on Kerr-AdS is also superradiantly unstable [26]. Later, this is extended to gravitational perturbation where hydrodynamic modes, quasinormal modes, and unstable superradiant modes are discussed [27]. We would like to refer the readers to Ref. [28] for an excellent review on superradiance and superradiant instability.

A new class of exact spherically symmetric neutral/charged black hole solutions in dRGT massive gravity was found in Ref. [16]. The effective cosmological constant naturally arises in the theory and can be written in terms of the graviton mass. One could treat these black holes as either modified Schwarzschild/Reissner-Nordström with a positive or negative cosmological constant depending on the choice of free parameters. In addition, scalar perturbation on neutral/charged dRGT black holes and their thermodynamic behavior are studied in Ref. [29]. A natural question that one might ask is whether these dRGT black holes experience superradiant phenomena. Could de Sitter (dS) and AdS boundaries lead to an instability caused by the superradiant effect? What is the effect of the massive charged scalar field on the charged dRGT black holes in asymptotically dS and AdS spacetimes?

The main purpose of this paper is to study the perturbation of the massive charged scalar field in the dRGT black hole spacetime. This is equivalent to the study of quasinormal modes (QNMs) of black holes in the scalar channel, with extension to the complex scalar perturbations. In contrast to the normal modes, QNMs decay/grow with complex frequencies that are uniquely determined by black hole's physical parameters, i.e., mass, charge, and angular momentum. The existence of the unique linear term in the metric of the dRGT model inevitably alters the QNMs of the charged scalar in such a background. We address such behavior in this paper. In Sec. II, we introduce the basic setup for constructing the charged black hole solution in dRGT massive gravity. Most of the details discussed in this section originate from the work done in Ref. [16]. Then, we discuss the effects of linear term (γ), which is the unique character of the black holes in dRGT massive gravity, in Sec. III. In Sec. IV, the Klein-Gordon equation of the massive charged scalar field on the dRGT black hole spacetime is derived. Then, the QNMs of dRGT black holes with a positive cosmological constant are explored in Sec. V. The QNMs of dRGT black holes with a negative cosmological constant are calculated in Sec. VI. In Sec. VII, we provide an analytic calculation for the diffusive modes (QNMs with a zero real part) of the dRGT background. Our conclusions are presented in Sec. VIII.

II. FORMALISM

The dRGT massive gravity coupled with the massive charged scalar field is described by the action [11] (with $c = 8\pi G = 1$)

$$S = \frac{1}{2}\int d^4x\sqrt{-g}[R + m_g^2\mathcal{U}(g,\phi^a) + \mathcal{L}_m], \tag{2}$$

where the matter Lagrangian is

$$\mathcal{L}_m \equiv \mathcal{L}_{\rm EM} + \mathcal{L}_\Phi, \\ = -\frac{1}{2}F_{\mu\nu}F^{\mu\nu} - g^{\mu\nu}D^*_{(\mu}\Phi^* D_{\nu)}\Phi - m_s^2\Phi^*\Phi. \quad (3)$$

Graviton mass and scalar field mass are denoted by m_g and m_s, respectively. The symmetrized combination of indices is defined as $X_{(\mu\nu)} = \frac{1}{2}(X_{\mu\nu} + X_{\nu\mu})$. The field strength tensor in the curved spacetime is given by $F_{\mu\nu} = A_{\nu;\mu} - A_{\mu;\nu}$, and the covariant derivative in the presence of the gauge symmetry is $D_\mu = \nabla_\mu - iqA_\mu$, where A_μ is the electromagnetic potential and q is the charge of the scalar field Φ.

The ghost-free massive graviton self-interacting potential is given by

$$\mathcal{U}(g, \phi^a) = \mathcal{U}_2 + \alpha_3\mathcal{U}_3 + \alpha_4\mathcal{U}_4, \quad (4)$$

where

$$\alpha_3 = \frac{\alpha - 1}{3}, \quad (5)$$

$$\alpha_4 = \frac{\beta}{4} + \frac{1-\alpha}{12}. \quad (6)$$

$$\mathcal{U}_2 = [\mathcal{K}]^2 - [\mathcal{K}^2], \quad (7)$$

$$\mathcal{U}_3 = [\mathcal{K}]^3 - 3[\mathcal{K}][\mathcal{K}^2] + 2[\mathcal{K}^3], \quad (8)$$

$$\mathcal{U}_4 = [\mathcal{K}]^4 - 6[\mathcal{K}]^2[\mathcal{K}^2] + 8[\mathcal{K}][\mathcal{K}^3] + 3[\mathcal{K}^2]^2 - 6[\mathcal{K}^4]. \quad (9)$$

α and β are free parameters. $\mathcal{K}^\mu_\nu = \delta^\mu_\nu - \sqrt{g^{\mu\sigma}f_{ab}\partial_\sigma\phi^a\partial_\nu\phi^b}$. $[\mathcal{K}] = \mathcal{K}^\mu_\mu$ and $[\mathcal{K}^n] = (\mathcal{K}^n)^\mu_\mu$. We will work in the unitary gauge for which the four Stückelberg fields take the form $\phi^a = x^\mu\delta^a_\mu$. The fiducial metric is chosen to be $f_{ab} = \mathrm{diag}(0, 0, c^2, c^2\sin^2\theta)$, where c is a constant.

A. Field equations

By varying (2), three equations of motions are obtained,

$$R_{\mu\nu} - \frac{1}{2}Rg_{\mu\nu} = -m_g^2 X_{\mu\nu} + (T^F_{\mu\nu} + T^\Phi_{\mu\nu}), \quad (10)$$

$$F^{\mu\nu}{}_{;\mu} = J^\nu, \quad (11)$$

$$D_a D^a\Phi = m_s^2\Phi, \quad (12)$$

where $X_{\mu\nu}$ is given by [16]

$$X_{\mu\nu} = \mathcal{K}_{\mu\nu} - \mathcal{K}g_{\mu\nu} - \alpha\left\{\mathcal{K}^2_{\mu\nu} - \mathcal{K}\mathcal{K}_{\mu\nu} + \frac{[\mathcal{K}]^2 - [\mathcal{K}^2]}{2}g_{\mu\nu}\right\} \\ + 3\beta\left\{\mathcal{K}^3_{\mu\nu} - \mathcal{K}\mathcal{K}^2_{\mu\nu} + \frac{1}{2}\mathcal{K}_{\mu\nu}\{[\mathcal{K}]^2 - [\mathcal{K}^2]\}\right\} \\ - \frac{1}{6}g_{\mu\nu}\{[\mathcal{K}]^3 - 3[\mathcal{K}][\mathcal{K}^2] + 2[\mathcal{K}^3]\}\Big\}. \quad (13)$$

The energy-momentum tensors of the gauge and scalar fields are

$$T^F_{\mu\nu} = F_{\mu\gamma}F_\nu{}^\gamma - \frac{1}{4}g_{\mu\nu}F_{\gamma\lambda}F^{\gamma\lambda} \quad (14)$$

$$T^\Phi_{\mu\nu} = D^*_{(\mu}\Phi^* D_{\nu)}\Phi + g_{\mu\nu}\mathcal{L}_\Phi. \quad (15)$$

Finally, the Noether current J^ν of the scalar field is

$$J^\nu = \frac{iq}{2}(\Phi^* D^\nu\Phi - \Phi(D^\nu\Phi)^*). \quad (16)$$

B. Black hole solutions

In the absence of a charged scalar field $T^\Phi_{\mu\nu} = 0$, the Einstein equations (10) admit a static spherically symmetric solution in the form [16]

$$ds^2 = -f(r)dt^2 + f^{-1}dr^2 + r^2d\theta^2 + r^2\sin^2\theta d\varphi^2, \quad (17)$$

where

$$f(r) = 1 - \frac{2M}{r} + \frac{Q^2}{r^2} - \frac{\Lambda}{3}r^2 + \gamma r + \epsilon, \quad (18)$$

$$\Lambda = -3m_g^2(1 + \alpha + \beta), \quad (19)$$

$$\gamma = -cm_g^2(1 + 2\alpha + 3\beta), \quad (20)$$

$$\epsilon = c^2m_g^2(\alpha + 3\beta). \quad (21)$$

The mass and electric charge of the black hole are denoted by M and Q, respectively, where ϵ is a constant. If $(1 + \alpha + \beta) > 0$, we obtain the modified Reissner-Nordström-AdS solution, while $(1 + \alpha + \beta) < 0$ yields the modified dS-type solution. In the limit $c \to 0$, which sets $\gamma = \epsilon = 0$, the metric (18) becomes the standard Reissner-Nordström solution with a cosmological constant. In addition, if the graviton mass is set to zero, we obtain the asymptotically flat Reissner-Nordström solution.

Apart from the parameters α and β parametrizing cubic and quartic graviton interactions, there are two main effects of massive gravity in the dRGT model reflected in two parameters: the graviton mass m_g and the parameter c in the fiducial metric $f_{ab} = \mathrm{diag}(0, 0, c^2, c^2\sin^2\theta)$. After setting ϵ to zero [30], all physical parameters in the metric (18) depend on m_g^2, but only γ, presenting a linear term in r,

depends on c. The cosmological constant Λ, on the other hand, does not depend on the fiducial metric parameter c. The two quantities Λ and γ are thus independent. We can have a massive-gravity model with $m_g \neq 0$ but vanishing c, which will lead to only the cosmological constant term in the metric, or we can have a massive-gravity model with nonzero c resulting in the existence of linear term γr in the metric in addition to the cosmological constant term.

III. EFFECTS OF γ PARAMETER

We will consider effects of the γ term unique in the massive-gravity model in this section. It will be shown for fixed physical parameters M, Q, Λ and $\epsilon = 0$ that varying γ could lead to spacetime with differing properties starting from regular spacetime to a black hole and extremal black hole. This is unique to the spacetime in massive-gravity theories. Since we expect flat spacetime with the usual radial coordinate centered at $r = 0$ due to spherical symmetry, it is reasonable to set $\epsilon = 0$, implying $\alpha = -3\beta$. We are thus left with two independent parameters, β and c. For a fixed value of graviton mass m_g^2, Λ and γ given by (19) and (20) remain independent.

A. Positive Λ

In general, the metric function (18) has four roots. It is possible that all the roots are real. More specifically, for the dS-type solution, there will be three positive roots and one negative root. All three positive roots will be treated as Cauchy horizon r_m, event horizon r_h, and cosmological horizon r_c, where $r_m < r_h < r_c$. The root structure of the metric function (18) is shown in Fig. 1. In this plot, we fix the black hole mass M, charge Q, cosmological constant Λ, and ϵ to be $M = 1$, $Q = 0.99$, $\Lambda = 0.01$, and 0, respectively. The four curves represent four different values of γ. With $\gamma = -0.1$ and $\gamma = 0$, these black holes have three real positive roots as shown in Fig. 1. The innermost zero is the black hole's inner horizon, whereas the second and the third (outermost) zeros are the black hole's event horizon and cosmological horizon, respectively. For $\gamma = 0.1$, there is only one horizon located at $r \approx 37.5$. More interestingly, with $\gamma = -0.2$, outside the horizon, the metric function f is always negative; hence, the spacetime structure *outside* its horizon is similar to the *inside* spacetime structure of the standard Schwarzschild black hole. One observes that as γ increases the metric function develops its second and third nodes. Therefore, we expect that an extremal case $(f'(r_h) = f(r_h) = 0)$ could exist at some point in the interval $0 < \gamma < 0.1$ as can be seen from Fig. 1.

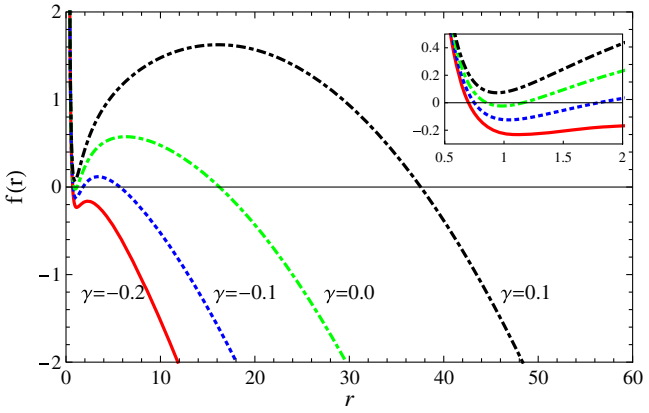

FIG. 1. The behavior of metric function $f(r)$ plotted against radius for various values of γ with fixed $M = 1, Q = 0.99$, $\Lambda = 0.01, \epsilon = 0$. A subplot shows the behavior of $f(r)$ when r is small.

B. Negative Λ

For negative cosmological constant Λ, the spacetime is asymptotically AdS. To be specific, we set the mass, charge, and cosmological constant term to be $M = 1$, $Q = 0.99$, and $\Lambda = -0.01$ and consider the effect of γ on the spacetime. As shown in Fig. 2, changing γ to a large positive value could turn a black hole spacetime into a regular spacetime with no horizon but with naked singularity at $r = 0$. At approximately $\gamma = 0.0175$, the black hole becomes extremal with the inner regular spacetime behind the horizon due to the charge contribution. For $0.0175 > \gamma > -0.1081$, we have a small black hole (with respect to $\sqrt{3/|\Lambda|}$). At $\gamma = -0.1081$, the black hole becomes extremal again with the regular inner region of spacetime behind the horizon. In contrast to the extremal black hole in conventional gravity where the charge contribution generates regular spacetime inside the horizon, this regular inner spacetime region originates from the massive-gravity *negative* γ contribution. For an even more negative value of $\gamma < -0.1081$, the black hole becomes large.

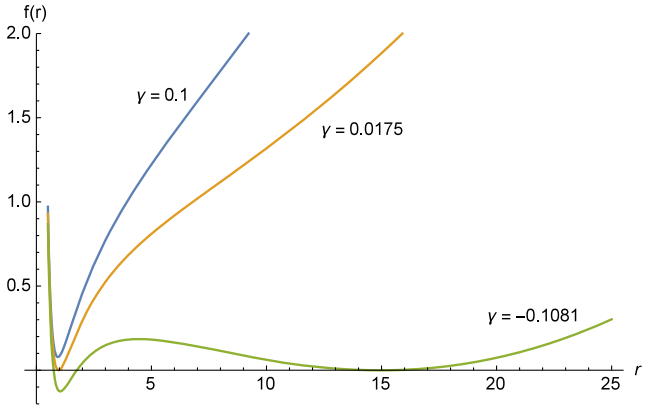

FIG. 2. The metric function $f(r)$ with differing values of γ. For demonstration, we set $M = 1$, $Q = 0.99$, $\Lambda = -0.01$, and $\epsilon = 0$. For $\gamma > 0.0175$, the spacetime becomes regular with no horizon. The spacetime contains an extremal black hole when $\gamma = 0.0175, -0.1081$. For $0.0175 > \gamma > -0.1081$, we have nonextremal black hole spacetime. When $\gamma < -0.1081$, the black hole becomes large with $r_h > \sqrt{3/|\Lambda|}$.

IV. LINEAR PERTURBATIONS IN ELECTROVACUUM

We shall now consider the massive charged scalar field propagating in the background (17). We assume there is no backreaction of the scalar field onto the spacetime geometry. The evolution of the charged scalar field can be described by the Klein-Gordon equation (12). Using the ansatz, $\Phi = e^{-i\omega t}\frac{\phi(r)}{r}Y(\theta,\varphi)$ with $Y(\theta,\varphi)$ the spherical harmonics and $A_\mu = \{A_0, 0, 0, 0\}$, the scalar field equation becomes separable between the radial and angular parts. The radial wave equation reads

$$f\phi'' + f'\phi' + \left(\frac{1}{f}(\omega + qA_0)^2 - \frac{\ell(\ell+1)}{r^2} - \frac{f'}{r} - m_s^2\right)\phi = 0, \tag{22}$$

where $f' = df/dr$ and $-\ell(\ell+1)$ is the eigenvalue of the angular operator. This equation (22) can be recast into the Schrödinger-like form

$$-\frac{d^2\phi}{dr_*^2} + \left[-(\omega + qA_0)^2 + f\left(m_s^2 + \frac{\ell(\ell+1)}{r^2} + \frac{f'}{r}\right)\right]\phi = 0, \tag{23}$$

where we have introduced the tortoise coordinate r_*,

$$\frac{dr_*}{dr} = \frac{1}{f}. \tag{24}$$

If $\Lambda < 0$, the tortoise coordinate is defined in the range $-\infty < r_* < \mathcal{C}$, where $r_* \to -\infty$ near the event horizon and at infinity $r_* \to \mathcal{C}$, where $\mathcal{C}$ is a positive constant. For the $\Lambda > 0$ case, $r_* \to -\infty, \infty$ as r approaches outer event horizon r_h and cosmological horizon r_c, respectively.

V. QNMS OF CHARGED SCALAR IN POSITIVE Λ SPACETIME

A. Boundary condition

In the vicinity of the event horizon and cosmological horizon, the general solution of (23) can be written as

$$\phi_{\rm in} \sim \begin{cases} e^{-i\tilde{\omega}r_*}, & \text{as } r \to r_h \\ C_1 e^{-i\hat{\omega}r_*} + C_2 e^{i\hat{\omega}r_*}, & \text{as } r \to r_c. \end{cases} \tag{25}$$

where $\tilde{\omega} \equiv (\omega + qA_h)$ and $\hat{\omega} \equiv (\omega + qA_c)$ for $A_h \equiv A_0(r_h)$ and $A_c \equiv A_0(r_c)$. Near the event horizon, there is no outgoing wave, whereas at the cosmic horizon, there are both ingoing and outgoing modes. This is the standard scattering problem in black hole physics.

For normal modes, the effective potential in (23) is real, and we can construct another linearly independent solution to (23) by taking the complex conjugate of (25). We thus define $\phi_{\rm out} = \phi_{\rm in}^*$. Then, we compute the Wronskian of these solutions by

$$W(\phi_{\rm in}, \phi_{\rm out}) = \phi_{\rm in}\frac{d\phi_{\rm out}}{dr_*} - \phi_{\rm out}\frac{d\phi_{\rm in}}{dr_*}. \tag{26}$$

Next, we obtain the following by evaluating the Wronskian at the event horizon and cosmological horizon:

$$W|_{r_*=-\infty} = 2i\tilde{\omega}, \tag{27}$$

$$W|_{r_*=\infty} = 2i\hat{\omega}(|C_1|^2 - |C_2|^2). \tag{28}$$

Since the Wronskian of linearly independent solutions must be a constant, we thus have

$$\frac{\tilde{\omega}}{\hat{\omega}}|T|^2 = 1 - |R|^2, \tag{29}$$

where we have defined

$$C_1 = \frac{1}{T}, \qquad \frac{C_2}{C_1} = R. \tag{30}$$

$|T|^2$ and $|R|^2$ are the transmission and reflection coefficients, respectively. One can see that if $|R| > 1$ then we must have $\frac{\tilde{\omega}}{\hat{\omega}} < 0$. This implies

$$\frac{qQ}{r_c} < \omega < \frac{qQ}{r_h}, \tag{31}$$

where we choose $A_0 = -Q/r$. If the frequency of the scalar field obeys this condition. then its reflection amplitude is greater than unity, and we thus have the superradiance effect. This result agrees with those found in Ref. [24], in which superradiance of charged scalar field on RN dS is investigated. Note that in the asymptotically flat limit, i.e., $r_c \to \infty$, this superradiant condition reduces to those in the standard RN case [19].

We shall now consider the quasinormal boundary condition. This is obtained by considering only the outgoing mode at the cosmological horizon. Thus, we have

$$\phi_{\rm in} \sim \begin{cases} e^{-i\tilde{\omega}r_*}, & \text{as } r \to r_h \\ e^{i\hat{\omega}r_*}, & \text{as } r \to r_c. \end{cases}, \tag{32}$$

The frequencies satisfying this boundary condition are called quasinormal frequencies [24,31,32]. This boundary condition implies that the frequencies ω are complex numbers. The scalar perturbation will be stable if $\mathrm{Im}(\omega) < 0$ (decaying). However, if $\mathrm{Im}(\omega) > 0$ (growing), we have unstable modes.

For the dS-type solution, we shall use the asymptotic iteration method (AIM) to compute the quasinormal modes. AIM was first developed for obtaining the solution of the second-order ordinary differential equations [33]. Also, AIM is applied to compute the QNMs of Schwarzschild and Schwarzschild-de Sitter black holes [34]. Recently, the authors of Ref. [29] used AIM to study the QNMs of black

holes in dRTG massive gravity. AIM is also used to study the QNMs of a charged Lifshitz black hole in Ref. [35].

B. Computation of QNMs using AIM

To calculate the quasinormal frequencies using AIM, it is convenient to make a change of variable $r = 1/x$. The radial part of the Klein-Gordon equation (22) becomes

$$\phi'' + \frac{p'}{p}\phi' + \left[\frac{(\omega - qQx)^2}{p^2} - \frac{1}{p}\left(\ell(\ell+1) + 2Mx - 2Q^2x^2 + \frac{\gamma}{x} - \frac{2\Lambda}{3x^2} + \frac{m_s^2}{x^2}\right)\right]\phi = 0, \tag{33}$$

where

$$p = Q^2x^4 - 2Mx^3 + (1+\epsilon)x^2 + \gamma x - \frac{\Lambda}{3}. \tag{34}$$

In this section, $'$ denotes a derivative with respect to x. It would be convenient to introduce [29,34,36]

$$e^{i\omega r_*} = (x-x_1)^{\frac{i\omega}{2\kappa_1}}(x-x_2)^{\frac{i\omega}{2\kappa_2}}(x-x_3)^{\frac{i\omega}{2\kappa_3}}(x-x_4)^{\frac{i\omega}{2\kappa_4}}, \tag{35}$$

where $x_i = 1/r_i$ for $i = 1, 2, 3, 4$, which represent each of the real roots of $f(r)$. The outer event horizon and cosmological horizon will be denoted by x_1 and x_2, whereas the inner event horizon and a negative real root are x_3 and x_4, respectively. We have also introduced the surface gravity, which is defined as

$$\kappa_i = \frac{1}{2}\left.\frac{df}{dr}\right|_{r\to r_i}. \tag{36}$$

For example, the surface gravity at the event horizon is denoted by κ_1. To scale out the divergent behavior at the cosmic horizon, we define

$$\phi(x) = e^{i\omega r_*}u(x). \tag{37}$$

The wave equation (33) therefore takes the following form:

$$u'' + \frac{(p' - 2i\omega)}{p}u' - \frac{1}{p}\left[\ell(\ell+1) + 2Mx - 2Q^2x^2 + \frac{\gamma}{x} - \frac{2\Lambda}{3x^2} + \frac{m_s^2}{x^2} + \frac{qQx}{p}(2\omega - qQx)\right]u. \tag{38}$$

In the absence of charge q and mass m_s of the scalar field, this equation becomes similar to that of Ref. [29]. At the event horizon, the divergent behavior is scaled out by taking

$$u(x) = (x-x_1)^{-\frac{i\omega}{\kappa_1}}\chi(x). \tag{39}$$

Finally, the radial equation becomes

$$\chi''(x) = \lambda_0(x)\chi'(x) + s_0(x)\chi(x), \tag{40}$$

with

$$\lambda_0 = -\frac{4i\omega}{Q^2(x-x_1)(x_1-x_2)(x_1-x_3)(x_1-x_4)} - \frac{p' - 2i\omega}{p}, \tag{41}$$

$$s_0 = \frac{\ell(\ell+1) + 2x(M - Q^2x)}{p} + \frac{2m_s^2 + 3\gamma x + 2\Lambda}{3px^2} + \frac{qQx(2\omega - qQx)}{p^2} - \frac{2i\omega p'}{pQ^2(x-x_1)(x_1-x_2)(x_1-x_3)(x_1-x_4)} - \frac{4\omega^2}{pQ^2(x-x_1)(x_1-x_2)(x_1-x_3)(x_1-x_4)} + \frac{4\omega^2}{Q^4(x-x_1)^2(x_1-x_2)^2(x_1-x_3)^2(x_1-x_4)^2} + \frac{2i\omega}{Q^2(x-x_1)^2(x_1-x_2)(x_1-x_3)(x_1-x_4)}. \tag{42}$$

By differentiating the above equation with respect to x for n times, we obtain [29]

$$\chi^{(n)} = \lambda_{n-2}\chi' + s_{n-2}\chi, \tag{43}$$

where the coefficients λ_{n-2} and s_{n-2} form a recurrent relation as

$$\lambda_n = \lambda'_{n-1} + \lambda_{n-1}\lambda_0 + s_{n-1}, \tag{44}$$

$$s_n = s'_{n-1} + s_0\lambda_{n-1}. \tag{45}$$

For sufficiently large n, the asymptotic behavior implies

$$\frac{s_n}{\lambda_n} = \frac{s_{n-1}}{\lambda_{n-1}} \equiv \beta, \tag{46}$$

where β is a constant. The quasinormal frequencies ω can be found from the quantization condition [34]

$$\lambda_n(x)s_{n-1}(x) = \lambda_{n-1}(x)s_n(x). \tag{47}$$

To obtain the energy eigenvalues, each coefficient will be constructed in terms of their previous iteration via (44)

and (45). This means each derivative of λ and s will also be determined. The quantization condition (47) will yield the expression for the energy eigenvalues. However, this becomes one of the main disadvantages of this method, since at each step one must calculate the derivative of λ and s of the previous iteration. This can be very time consuming and also affects the precision of the numerical calculation [29,34]. To avoid this problem, an improved version of AIM has been proposed by the authors of Ref. [34]. The improved AIM overcomes the need to take the derivative at each iteration by expanding λ_n and s_n in a Taylor series around the point $\bar{x}$,

$$\lambda_n(\bar{x}) = \sum_{i=0}^{\infty} c_n^i (x-\bar{x})^i, \tag{48}$$

$$s_n(\bar{x}) = \sum_{i=0}^{\infty} d_n^i (x-\bar{x})^i, \tag{49}$$

where c_n^i and d_n^i are the ith Taylor coefficients of λ_n and s_n. Inserting these expressions into (44) and (45), we obtain

$$c_n^i = (i+1)c_{n-1}^{i+1} + d_{n-1}^i + \sum_{k=0}^{i} c_0^k c_{n-1}^{i-k}, \tag{50}$$

$$d_n^i = (i+1)d_{n-1}^{i+1} + \sum_{k=0}^{i} d_0^k c_{n-1}^{i-k}. \tag{51}$$

The quantization condition (47) can be now expressed in terms of these new recursion relations:

$$d_n^0 c_{n-1}^0 - d_{n-1}^0 c_n^0 = 0. \tag{52}$$

Thus, the improved AIM does not need the derivative operator. The quasinormal frequency can be obtained by solving a set of recursion relations above. The computational steps are as follows. First, the coefficients c_n^i and d_n^i are computed via (50) and (51) starting from $n = 0$ and iterating up to $n + 1$ until the desired number of recursions is reached. Then, at each iteration n, the coefficients are determined with $i < N - n$, where N is the maximum number of iterations, since the quantization condition (52) contains only $i = 0$. In this paper, for the asymptotically de Sitter solution, we will calculate the quasinormal mode of the dRGT charged black hole using the improved AIM.

C. Results

The QNMs of the dRGT massive-gravity de Sitter black hole are calculated by *Mathematica*'s notebook adopted from Ref. [37]. In Table I, we calculate the QNMs for massless charged scalar perturbation for various values of γ. The location of the black hole event horizon x_1 and the cosmic horizon x_2 change as γ is varied. In this table, we show three sets of quasinormal frequencies ω distinguished by the expansion point $\bar{x}$. We display the three lowest modes of the imaginary part for each fixed γ. In each case, we find that the lowest mode becomes the normal mode,

TABLE I. The QNMs for massless charged scalar perturbations of a charged dRGT black hole for $M = 1$, $Q = 0.5$, $\Lambda = 0.01, q = 0.99, \epsilon = 0, \ell = 0$. Note that the number of iterations for the $\bar{x} = \frac{x_1+x_2}{2}$ case is 180.

QNMs calculated by improved AIM (100 iterations)					
γ	$\omega(\bar{x} = 0.3x_1)$	$\omega(\bar{x} = 0.9x_1)$	$\omega(\bar{x} = \frac{x_1+x_2}{2})$	qQ/r_c	qQ/r_h
−0.10	$0.045713 + 5.52 \times 10^{-14}i$ $0.045713 - 0.035508i$ $0.045713 - 0.071017i$	$0.091473 - 7.06 \times 10^{-15}i$ $0.091473 - 0.064954i$ $0.091473 - 0.129908i$	$0.027331 + 0.009470i$ $0.067230 + 0.013379i$ $0.046779 + 0.013992i$ $0.089034 + 0.017426i$ $0.125727 + 0.018862i$	0.091427	0.182945
−0.05	$0.025576 - 1.85 \times 10^{-15}i$ $0.025576 - 0.046854i$ $0.025576 - 0.093707i$	$0.115275 - 6.41 \times 10^{-13}i$ $0.115275 - 0.159514i$ $0.115275 - 0.319028i$	$0.049368 + 0.012092i$ $0.115124 + 0.036522i$	0.051152	0.230550
0.00	$0.015253 + 4.96 \times 10^{-15}i$ $0.015253 - 0.050350i$ $0.015253 - 0.100700i$	$0.130935 - 1.07 \times 10^{-12}i$ $0.130935 - 0.236556i$ $0.130935 - 0.473111i$	$0.021209 + 0.010103i$ $0.106157 + 0.042381i$	0.030505	0.261869
0.05	$0.009612 + 1.97 \times 10^{-10}i$ $0.009612 - 0.059340i$ $0.009612 - 0.118680i$	$0.143604 + 4.92 \times 10^{-13}i$ $0.143604 - 0.307075i$ $0.143604 - 0.614150i$	$0.007692 + 0.007593i$ $0.096506 + 0.043602i$	0.019223	0.287208
0.10	$0.006619 + 1.93 \times 10^{-6}i$ $0.006575 - 0.074538i$ $0.006590 - 0.149093i$	$0.154574 + 5.68 \times 10^{-13}i$ $0.154574 - 0.373815i$ $0.154574 - 0.747629i$	$0.002261 + 0.086304i$ $0.086305 + 0.042360i$	0.013178	0.309148

i.e., zero imaginary part, while the real part is nonzero. Moreover, as the imaginary part increases (in magnitude), the real part of ω remains unchanged. The step of change in the imaginary part for the same real part is also found to be constant. These modes are the diffusive QNMs of the uncharged black hole being shifted by Coulomb energy when the scalar charge q is turned on. We also observe that as γ increases the real part of ω decreases, while the imaginary part of ω increases (in magnitude) when $\bar{x} = 0.3x_1$. For the near-horizon solution ($\bar{x} = 0.9x_1$), as γ increases, both the real part and imaginary part increase. For the expansion point $\bar{x} = 0.3x_1$, these modes live outside the superradiant regime, while all the results from another point ($\bar{x} = 0.9x_1$) satisfy the superradiant condition (31). Since we have found only QNMs with $\mathrm{Im}(\omega) < 0$, these modes are stable.

However, unstable modes are found when the expansion point is $\bar{x} = \frac{x_1+x_2}{2}$. Note that the unstable QNMs obtained from the AIM converge relatively slowly when compared to the stable one. It can be seen from Table I that for a given γ only the most unstable modes live in the superradiant regime. Therefore, not all the unstable modes discovered here are superradiant. For the QNMs of RN dS [23], only $\ell = 0$ modes are unstable, and the nature of this instability is due to the superradiance effect [24]. Moreover, even though all the unstable modes found in Refs. [24] (for RN dS) are superradiant, not all the superradiant modes are unstable.

A remarkable aspect of the results is the existence of three kinds of solutions categorized by $\bar{x}$, the near-r_h, the near-r_c, and the all-region solutions. The near-$r_h(r_c)$ solution uses $\bar{x}$ close to the event horizon (cosmic horizon) at $x_1(x_2)$, and the all-region solution uses $\bar{x}$ in the intermediate region between the two horizons. In Table I, the near-r_h (r_c) solution is given by AIM for $\bar{x} = 0.9x_1(0.3x_1)$. Each near-horizon solution is separated by the potential wall in the background, and they have relatively smaller energies [denoted by $\mathrm{Re}(\omega)$] than the potential wall. They are thus confined within the near-horizon regions with the wave function exponentially suppressed in the intermediate region where the potential wall dominates. These modes found in the near-horizon regions have identical real parts determined by quantity $qQ/2r_h(qQ/2r_c)$ as shown in Table I. In fact, we observe that all the real parts for the near-horizon solutions in Tables II–IV are equal to these factors. We can understand the shift in $\mathrm{Re}(\omega)$ (i.e., energy) for the charged QNMs of these modes as the electric potential energy generated from the Coulomb interaction between the charged scalar and the charged black hole. Table III confirms this relationship; the value of $\mathrm{Re}(\omega)$ is proportional to q for a fixed Q, and it is equal to $qQ/2r_h(qQ/2r_c)$. Therefore, we can conclude that these near-horizon modes correspond to the diffusive QNMs of the uncharged black hole being shifted (in the real parts) by the electric potential when the charge of the scalar field is turned on.

On the other hand, the all-region solution has energy higher than the potential wall, and thus the QNMs of the all-region solution have much higher $\mathrm{Re}(\omega)$ as shown in Tables II–IV (exceptions are the unstable modes found in Table I, in which the energies could become relatively small but still higher than the potential wall). These QNMs in all-region solutions are to be compared with values from the Wentzel-Kramers-Brillouin (WKB) method since WKB finds the quantization condition from connecting solutions from the two regions around the maximum of the potential.

The effect of cosmological constant Λ on the QNMs of charged black holes is shown in Table II. For each fixed Λ, we show the three lowest modes of the quasinormal frequencies. With fixed Λ, we find a normal mode as the lowest possible mode. For the expansion point far from the black hole's horizon $\bar{x} = 0.3x_1$, the real part and the imaginary part of the quasinormal frequencies increase as the cosmological constant increases. For the near-horizon point $\bar{x} = 0.9x_1$, the real part and the imaginary part of ω decrease as Λ increases. It is interesting that the imaginary part of QNMs with the same real part at each Λ increases by a constant step for each evaluating point $\bar{x} = 0.3x_1, 0.9x_1$. As discussed above, these QNMs are the diffusive modes of

TABLE II. The QNMs for charged scalar perturbations of a charged dRGT black hole for $M = 1$, $Q = 0.9, \gamma = 0.02$, $q = 0.1, m_s = 0.2, \ell = 2, \epsilon = 0$.

QNMs calculated by improved AIM (100 iterations)				
Λ	$\omega(\bar{x} = 0.3x_1)$	$\omega(\bar{x} = 0.9x_1)$	$\omega(\bar{x} = \frac{x_1+x_2}{2})$	Third-order WKB ($n = 0$)
0.01	$0.002283 + 2.27 \times 10^{-9}i$ $0.002283 - 0.053227i$ $0.002289 - 0.106455i$	$0.032466 - 3.03 \times 10^{-12}i$ $0.032466 - 0.221712i$ $0.032466 - 0.443424i$	$0.662813 - 0.101124i$	$0.661603 - 0.102322i$
0.05	$0.006169 + 5.63 \times 10^{-13}i$ $0.006169 - 0.094880i$ $0.006169 - 0.189760i$	$0.031029 + 2.94 \times 10^{-12}i$ $0.031029 - 0.195734i$ $0.031029 - 0.391468i$	$0.583884 - 0.089959i$	$0.582789 - 0.091289i$
0.1	$0.009885 - 6.11 \times 10^{-15}i$ $0.009885 - 0.102078i$ $0.009885 - 0.204156i$	$0.028898 - 3.67 \times 10^{-13}i$ $0.028898 - 0.155973i$ $0.028898 - 0.311945i$	$0.469468 - 0.072041i$	$0.468375 - 0.073434i$

TABLE III. The QNMs for charged scalar perturbations of a charged dRGT black hole for $M = 1$, $Q = 0.9, \gamma = 0.02, \Lambda = 0.09$, $m_s = 0.2, \ell = 2, \epsilon = 0$. The black hole event horizon is at $x_1 = 0.652566$, and the cosmic horizon is at $x_2 = 0.203419$.

	QNMs calculated by improved AIM (100 iterations)			
q	$\omega(\bar{x} = 0.3x_1)$	$\omega(\bar{x} = 0.9x_1)$	$\omega(\bar{x} = \frac{x_1+x_2}{2})$	Third-order WKB ($n = 0$)
0.1	$0.009154 + 1.32 \times 10^{-15}i$ $0.009154 - 0.102917i$ $0.009153 - 0.205834i$	$0.029365 - 3.56 \times 10^{-12}i$ $0.029366 - 0.164779i$ $0.029366 - 0.329558i$	$0.494253 - 0.076035i$	$0.493193 - 0.077453i$
0.2	$0.018308 + 1.77 \times 10^{-15}i$ $0.018308 - 0.102917i$ $0.018308 - 0.205834i$	$0.058731 + 1.39 \times 10^{-8}i$ $0.058734 - 0.164776i$ $0.058505 - 0.329645i$	$0.537927 - 0.077051i$	$0.535105 - 0.078125i$
0.3	$0.027462 + 8.78 \times 10^{-15}i$ $0.027462 - 0.102917i$ $0.027462 - 0.205834i$	$0.088096 - 2.24 \times 10^{-12}i$ $0.088096 - 0.164779i$ $0.088097 - 0.329558i$	$0.581910 - 0.079698i$	$0.577703 - 0.078755i$
0.4	$0.036615 - 3.00 \times 10^{-15}i$ $0.036616 - 0.102917i$ $0.036616 - 0.205834i$	$0.117462 - 1.57 \times 10^{-12}i$ $0.117462 - 0.164779i$ $0.117462 - 0.329558i$	$0.625336 - 0.083623i$	$0.620969 - 0.079346i$

TABLE IV. The QNMs for scalar perturbations of a charged dRGT black hole for $M = 1$, $Q = 0.5, \gamma = -0.8, \Lambda = 0.08, q = 0$, $\ell = 2, \epsilon = 1.984$. The black hole event horizon is at $x_1 = 1.501496$, and the cosmic horizon is at $x_2 = 0.386506$. Note that the number of iterations for the $\bar{x} = 0.9x_1$ case is 180.

	QNMs calculated by improved AIM (100 iterations)				
m_s	$\omega(\bar{x} = 0.3x_1)$	$\omega(\bar{x} = 0.9x_1)$	$\omega_0(\bar{x} = 0.6x_1)$	$\omega_1(\bar{x} = 0.6x_1)$	Third-order WKB ($n=0$)
0.00	$-1.06\times10^{-18}-0.341129i$ $6.78\times10^{-19}-0.663874i$ $-1.27\times10^{-18}-1.035320i$	$-3.08\times10^{-6}-0.996799i$ $5.99\times10^{-6}-1.977313i$ $-0.000029-2.967228i$	$2.43\times10^{-17}-0.725025i$ $-1.10\times10^{-15}-1.248286i$ $-1.94\times10^{-14}-1.733901i$	$1.597654-0.429275i$	$1.594307-0.429759i$
0.25	$-2.26\times10^{-18}-0.346144i$ $-1.42\times10^{-18}-0.677923i$ $-1.25\times10^{-19}-1.029516i$	$-2.93\times10^{-6}-0.997271i$ $4.88\times10^{-6}-1.976085i$ $-3.83\times10^{-6}-2.984651i$	$4.18\times10^{-17}-0.778603i$ $-1.62\times10^{-15}-1.268964i$ $-2.99\times10^{-14}-1.746501i$	$1.604779-0.427158i$	$1.601012-0.427723i$
0.50	$1.72\times10^{-18}-0.330507i$ $8.38\times10^{-18}-0.622042i$ $1.24\times10^{-18}-1.001285i$	$-3.73\times10^{-6}-0.996825i$ $0.000015-1.983883i$ $-6.81\times10^{-6}-2.984021i$	$4.13\times10^{-16}-0.994794i$ $-3.68\times10^{-15}-1.277465i$ $-6.49\times10^{-14}-1.781237i$	$1.625617-0.421757i$	$1.621181-0.421667i$

the scalar field in uncharged black hole background being shifted by the Coulomb energy when the scalar charge q is turned on. We also compute the QNMs by using the third-order WKB approximation (see Appendix for details). The results from WKB and AIM are compared, and we have used another expansion point $\bar{x} = \frac{x_1+x_2}{2}$ [38]. The results from two methods agree quite well with the difference only being about 0.1%. Similar to the results displayed in Table I, we find that some of theses frequencies satisfy the superradiant condition (with $\bar{x} = 0.9x_1$). In addition, we find no unstable mode since these modes exist with $\mathrm{Im}(\omega) < 0$.

In Table III, the effect of the scalar field charge q on the QNMs of charged black holes is shown. In this case, the black hole event horizon is located at $x_1 = 0.652566$, and the cosmological horizon is located at $x_2 = 0.203419$. For both sets of quasinormal frequencies, the real part $\mathrm{Re}(\omega)$ increases as the scalar charge q increases. However, increasing q does not affect the imaginary part of the quasinormal frequency. We notice that as q increases the real part of quasinormal frequencies is shifted up with the constant interval, which is 0.009154 for the first $\bar{x}$ and 0.029365 for the second $\bar{x}$. The Coulomb shifts are simply $qQ/2r_h$ for $\bar{x}$ near the event horizon and $qQ/2r_c$ for $\bar{x}$ near the cosmic horizon. For the all-region solutions using $\bar{x}$ in the intermediate region, WKB and AIM both give quasinormal frequencies that are in close agreement with each other. Some of these frequencies, i.e., mode with $\bar{x} = 0.9x_1$, live in the superradiant regime where this can be seen by checking whether the real part of ω is satisfied by the condition (31).

The QNMs for massive neutral scalar perturbations of a charged black hole in massive-gravity background are displayed in Table IV. We show the results by varying the scalar field mass m_s for 0, 0.25, and 0.50. As in all previous tables, the QNMs are shown with three different evaluating points. Note that the all-region solution is

computed using $\bar{x} = 0.6x_1 \approx \frac{x_1+x_2}{2}$. One distinguished feature of this table is that at $\bar{x} = 0.6x_1$ we obtain two branches of quasinormal frequencies. In the first branch ω_0, we show only three lowest modes of the quasinormal frequencies. In this branch, the real part of ω is zero, which means that these modes are purely decayed or growing. Moreover, increasing the scalar field mass m_s slightly increases the imaginary part of ω. For another branch we dub as ω_1, we find only one converged result for each fixed m_s. We see that ω_1 is in close agreement with the results obtained from the WKB method. In this branch, as m_s increases, the real part of ω also increases monotonically, and the imaginary part decreases. For the near-$r_h(r_c)$ solution, the diffusive modes are also obtained. We display the lowest possible value of the real part for the near-$r_h(r_c)$ solution. Despite some of these real parts being not exactly zero, they are the actual diffusive modes. These nonzero real parts could be resolved by increasing the number of iterations. It should not be surprising that some of these modes acquire a negative real part. This is because when $q = 0$ the equation of motion (33) has a symmetry under $\omega \to -\omega$. The effect of the scalar field mass on an imaginary part of ω is not straightforward for the near-$r_h(r_c)$ solution. One final remark is that we find that these diffusive modes are shifted from the real axis when the scalar charge q is switched on. The real parts will be shifted up with a factor $qQ/2r_h(qQ/2r_c)$ as we increase q in a way similar to that found in Table III.

VI. QNMS OF CHARGED SCALAR IN NEGATIVE Λ SPACETIME

In this section, we will consider the stability of the black hole in the current massive-gravity model when $\Lambda < 0$. The boundary condition at the event horizon is the ingoing waves and at spatial infinity is zero. In this case, Eq. (23) reduces to

$$\frac{d^2\phi}{dr_*^2} = -(\omega + qA_0)^2\phi, \tag{53}$$

for $f(r) \approx 0$ near the horizon $r \simeq r_h$. In this region, the scalar field takes the form

$$\phi(r) = Ae^{-i(\omega+qA_h)r_*} \equiv Ae^{-i\tilde{\omega}r_*}, \tag{54}$$

where $A_h = k + V_0/r_h$. Since

$$r_* = \int f^{-1}dr \simeq \frac{1}{f'(r_h)}\ln|r - r_h|, \tag{55}$$

we can rewrite the field in the near-horizon region in the form

$$\phi = f(r)^{-i\tilde{\omega}/4\pi T}(a_0 + a_1(r-r_h) + a_2(r-r_h)^2 + \cdots), \tag{56}$$

where T is the Hawking temperature.

As we approach $r \to \infty$, the equation of motion becomes

$$\frac{d^2\phi}{dr_*^2} = \left(m_s^2 - \frac{2\Lambda}{3}\right)\frac{\Lambda r^2}{3}\phi. \tag{57}$$

The solution of the scalar field in the far-away region is thus

$$\phi(r) = Br^{\alpha}, \tag{58}$$

where

$$\alpha = -\frac{1}{2}\left(1 \mp \sqrt{9 - \frac{12m_s^2}{\Lambda}}\right). \tag{59}$$

We will choose only the plus sign since we need the field to vanish at infinity. On the other hand, there is a class of solution that also vanishes at infinity for the minus sign choice of (59). It is simply required that $m_s^2/\Lambda > 2/3$. Interestingly, for $\Lambda < 0$, the possibility of negative mass square $m_s^2 < 0$ is also allowed as long as it satisfies the above requirement.

To solve for the QNMs of the charged scalar in the massive-gravity background, we rewrite the equation of motion (23) as

$$\frac{[(w+\mu(1-z))^2 - f(z)(-z^3f'(z) + \ell(\ell+1)z^2 + \tilde{m}^2)]\phi(z)}{f(z)} + z^2\frac{\partial}{\partial z}\left(z^2f(z)\frac{\partial\phi(z)}{\partial z}\right) = 0, \tag{60}$$

where we define $z = r_h/r, w = \omega r_h, \tilde{m} = m_s r_h$. With respect to the new coordinate, the physical region is $z \in [0, 1]$, the infinity is at $z = 0$, and the horizon is at $z = 1$. The electric potential is also expressed as

$$qA_0 = \mu\left(\frac{1}{r_h} - \frac{1}{r}\right), \tag{61}$$

where $\mu = qQ$. With this choice of gauge, the potential is set to ground at the horizon. To calculate the QNM frequencies, we linearize the equation of motion with respect to w by substituting [Eq. (62)] into (60) to obtain

$$\phi(z) = e^{-iwr_*}S(z), \tag{62}$$

$$\frac{[(2\mu w(1-z) + (\mu(1-z))^2) - f(z)(-z^3f'(z) + \ell(\ell+1)z^2 + \tilde{m}^2)]S(z)}{f(z)} + z^2\frac{\partial}{\partial z}\left(z^2f(z)\frac{\partial S(z)}{\partial z}\right) + 2iwz^2\frac{\partial S(z)}{\partial z} = 0. \tag{63}$$

Alternatively, we can work in the Eddington-Finkelstein coordinates $v \equiv t + r_*$ and obtain the equation of motion for the scalar field,

$$-(-z^3 f'(z) + \ell(\ell+1)z^2 + \tilde{m}^2 + i\mu z^2)\Psi(z) + z^2 \frac{\partial}{\partial z}\left(z^2 f(z)\frac{\partial \Psi(z)}{\partial z}\right) + 2iz^2(\mu(1-z)+w)\frac{\partial \Psi(z)}{\partial z} = 0, \tag{64}$$

which is automatically linear in w. Equations (63) and (64) are identical for $\mu = 0$. Generically, however, even when μ is nonzero, we expect the quasinormal frequencies calculated from both equations to be the same. We have numerically verified that the two equations of motion indeed give the same quasinormal frequencies.

Expanding for positive integer N

$$S(z) = \sum_{n=0}^{N} b_n T_n(2z-1), \tag{65}$$

where T_n is the Chebyshev polynomials of the first kind, we obtain the linear equation of coefficients b_n. In the limit $N \to \infty$, the expansion will be exact due to the completeness of the orthonormal Chebyshev polynomials in domain $[-1, 1]$. To compute the quasinormal frequencies, we adopt the spectral method by dividing the domain of interest $(2z-1) \in [-1, 1]$ into a finite number of grid points and solve the system of linear equations of coefficients b_n. The choice of grid points we adopt is the Gauss-Lobatto grid points

$$z_k = \frac{1}{2}\left(1 + \cos\left(\frac{k\pi}{N}\right)\right), \tag{66}$$

where $k = 0, 1, .., N$. The resulting system of linear equations is a generalized eigenvalue problem that can be solved to obtain the quasinormal frequencies w for a given N. The *Mathematica* code we used is adopted from Yaffe's method in Ref. [39].

A. Small AdS black hole

We will start with the set of physical parameters that gives the small AdS black hole. The parameter set we will use is a near-extremal black hole in conventional gravity, $M = 1, Q = 0.99, \Lambda = -0.01$.

The QNMs of the massless neutral scalar are shown in Fig. 3 for the angular momentum states $\ell = 0, 1, 2$. Similar to the QNMs of fluctuations in the black brane geometry, the QNMs show approximate asymptotic linearity in both real and imagniary parts (also previously shown in Ref. [40]). For $\ell = 0, 1$, there are "diffusive" or "hydrodynamic" modes with zero real parts, another characteristic that is similar to the QNMs of the black brane spacetime.

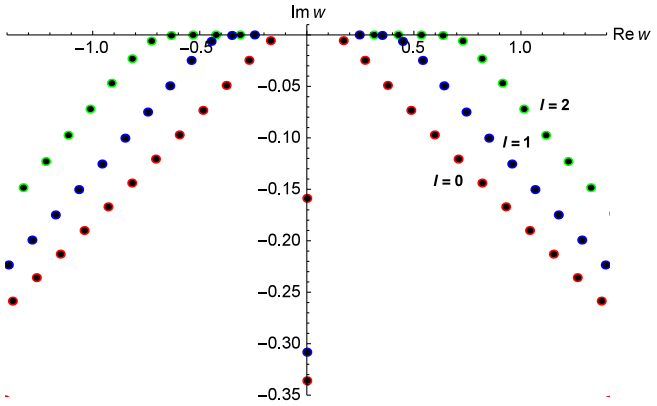

FIG. 3. The lowest QNMs $w = \omega r_h$ for $M = 1, Q = 0.99$, $\Lambda = -0.01, \gamma = 0, \mu = 0, m_s = 0, \ell = 0,\ 1,\ 2$. The red/black (blue/black, green/black) dots are for $\ell = 0(1, 2)$ when $N = 200/300$. The convergence of the results is excellent, as we can see no distinctive differences in the values of QNMs between $N = 200$ and $N = 300$.

The effect of the massive-gravity γ parameter is shown in Fig. 4. For diffusive modes with only imaginary parts, positive γ generates more diffusive quasinormal frequencies with smaller values. Analytic calculation of these modes is presented in Sec. VII. Smaller diffusive QNMs imply a longer relaxation time due to the massive-gravity paramater γ. For other QNMs with nonzero real parts, positive γ slightly increases the slope of the asymptotic line, i.e., reducing the corresponding energy of each QNM, while keeping the imaginary part mostly unchanged.

Figure 5 shows unstable QNMs when the black hole has charge opposite that of the scalar particle, i.e., $\mu = qQ < 0$, as we can see from the positive imaginary parts of w for positive energy $\mathrm{Re}(w) > 0$. The massive-gravity parameter γ does not affect the instability in a significant way as long as it does not change the background spacetime as mentioned above. It only lowers the energy of the scalar in the unstable modes. Using results of Ref. [41], after shifting the electric potential at the horizon by qQ/r_h to

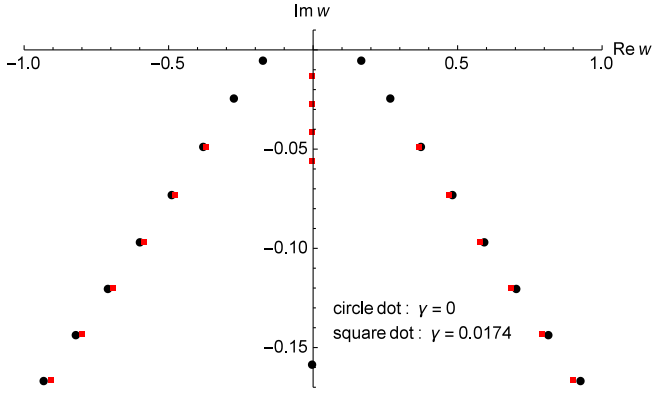

FIG. 4. The lowest QNMs $w = \omega r_h$ for $M = 1, Q = 0.99$, $\Lambda = -0.01, \mu = 0, \ell = 0, m_s = 0$ for $\gamma = 0,\ 0.0174$.

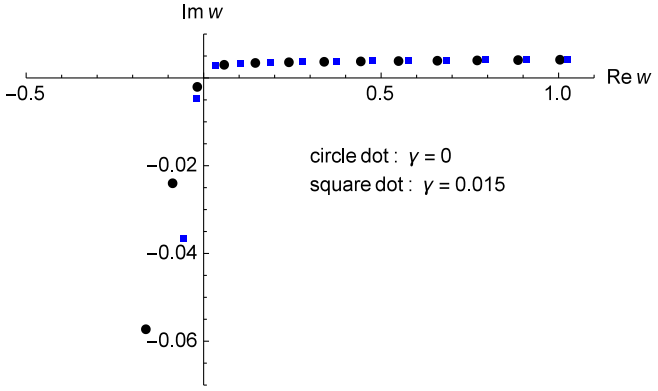

FIG. 5. The lowest QNMs $w = \omega r_h$ for $M = 1, Q = 0.99$, $\Lambda = -0.01, \mu = -2, \ell = 0, m_s = 0$ for $\gamma = 0,\ 0.015$.

make ground voltage at the horizon, superradiant modes are the QNMs with $\mathrm{Re}(\omega) < 0$ for $\mu = qQ > 0$. This is equivalent to the QNMs with $\mathrm{Re}(\omega) > 0$ for $\mu < 0$ since the equation of motion (22) depends on $(\omega + qA_h)^2$ and has thus a symmetry under $\omega \leftrightarrow -\omega, q \leftrightarrow -q$. Therefore, we can conclude that the unstable QNMs found are superradiant modes.

One possible interpretation of the unstable modes in the bulk is that the scalar will condensate around the black hole horizon, resulting in a superconducting layer outside the horizon [42]. Holographically, this would correspond to the superconducting phase of gauge theory on the AdS boundary. From the viewpoint of holographic duality, the electric potential at the AdS boundary can be identified with the chemical potential of the dual gauge matter living on the boundary. We found that sufficiently large $|\mu|$ causes instability of the bulk scalar profile. This could be interpreted as the instability of the boundary dual matter phase to condensation. It is possible that this is the condensation of scalar charged (quasi)particles on the boundary rendering a superconducting phase [42]. Interestingly, the diffusive modes with zero real parts disappear once the chemical potential μ is turned on.

B. Large AdS black hole

For a sufficiently large negative value of γ, e.g., $\gamma < -0.1081$ with $M = 1, Q = 0.99, \Lambda = -0.01$, the black hole turns into a *large* AdS black hole with $r_h \gtrsim R_{\mathrm{AdS}} = \sqrt{3/|\Lambda|} = 17.32$. Remarkably, the QNMs become almost purely diffusive for the massless uncharged scalar $(m_s = 0, \mu = 0)$ for $\ell = 0,\ 1,\ 2$ as shown in Table V. Other modes with nonzero real parts are nonconverging at least up to $N = 600$. At $\gamma = -0.6$, the AdS black hole has a large size with $r_h/R_{\mathrm{AdS}} = 10.3$. The two lowest modes that can be obtained with reliable convengence for $N = 600$ appear to be on the imaginary axis with very small real parts, and the imaginary parts are almost identical between the states with $\ell = 0,\ 1,\ 2$. The oscillations are damped overcritically away with nearly zero frequencies. Turning on the scalar charge, $\mu \neq 0$, does not change the results much; the first diffusive modes shift slowly to smaller imaginary values, while the second diffusive modes disappear. The convergence becomes very slow even at $N = 600$. For the $\ell = 0$ state, turning on μ shifts the diffusive mode away from the imaginary axis.

It is curious that the QNMs of scalar perturbations in the large black hole in asymptotically AdS background in the massive-gravity model (sufficiently large negative γ) become almost extinct with only few converging diffusive modes remaining. This phenomenon is purely massive-gravity effect. For a black hole in conventional gravity with the same mass and charge ($M = 1$, $Q = 0.99$, $\gamma = 0$, $\Lambda = -0.01$), the horizon radius given by $r_h = 1.121 \ll R_{\mathrm{AdS}}$ shows that it is a small AdS black hole. As shown in Figs. 3 and 4, this small AdS black hole has series of QNMs of scalar perturbations. Turning on massive-gravity parameter γ to a large negative value changes a small AdS black hole into a large one. As a result, most QNMs disappear with few diffusive modes surviving.

To complete the picture, we present QNMs of the scalar field in the large AdS black hole spacetime in conventional gravity without a massive graviton for $M = 100, Q = 9$, $\Lambda = -0.01$ in Table VI (we need to change the mass and charge since in Einstein gravity the parameter set $M = 1$, $Q = 0.99$ will always give a small AdS black hole or no black hole for $\Lambda < 0$). The convergence is very slow, and only a few reliably converging modes are found. In contrast to a large AdS black hole in massive gravity, the lowest QNMs have nonzero real parts, and there are no diffusive modes found (at least for this set of parameters). QNMs of a large AdS black hole in conventional gravity are intrinsically different from the QNMs of a large AdS black hole induced by pure massive-gravity effects (from an otherwise small AdS black hole in Einstein gravity).

It is possible that the very slow convergence of QNMs is partially an artifact of the numerical method we are using in this article. A different method, e.g., the Frobenius mothod [43], might reveal more converging QNMs for a large AdS black hole, even the one induced by massive-gravity effects

TABLE V. The lowest QNMs $w = \omega r_h$ for $M = 1, Q = 0.99, \Lambda = -0.01, \mu = 0, m_s = 0$ for $\gamma = -0.6$ and $\ell = 0$, 1, 2. The number of grid points is $N = 600$. The black hole is large with $r_h/R_{\mathrm{AdS}} = 10.3$.

n	$\ell = 0$	$\ell = 1$	$\ell = 2$
1	$2.28 \times 10^{-8} - 78.571056i$	$-3.51 \times 10^{-8} - 79.138264i$	$-2.42 \times 10^{-8} - 80.283881i$
2	$-0.0667 - 139.779252i$	$0.039062 - 140.051228i$	$0.046945 - 140.4673596i$

TABLE VI. The lowest QNMs $w = \omega r_h$ for $M = 100, Q = 9, \Lambda = -0.01, \mu = 0, m_s = 0$ for conventional gravity with $\gamma = 0$ and $\ell = 0$, 1, 2. The number of grid points is $N = 600$. The black hole is large with $r_h/R_{\mathrm{AdS}} = 2.1$.

n	$\ell = 0$	$\ell = 1$	$\ell = 2$
1	$\pm 9.208525 - 11.853083i$	$\pm 9.928185 - 11.635843i$	$\pm 11.165467 - 11.293674i$
2	$-15.404565 - 21.206122i$	$-16.178184 - 21.188500i$	$-16.933504 - 20.997096i$
	$16.722404 - 21.409218i$	$16.955786 - 21.151278i$	$16.369064 - 21.117862i$

under consideration. To check the converging aspect of our code with respect to the QNMs of a large AdS black hole, we compare results with previous work [43,44]. By numerically calculating the QNMs of scalar perturbation in a large AdS black hole spacetime with $M = 100, \Lambda = -0.01$, and other parameters equal to zero (this is a large AdS black hole with $r_h/R_{\mathrm{AdS}} = 2.11$), we found only the first converging modes ($n = 1, w = \pm 9.333909 - 11.918457i$) and the slowly converging second modes ($n = 2, w \simeq \pm 15 - 22i$) even at $N = 600$. This demonstrates a limitation on the converging aspect of our code when applied to a large AdS black hole with the full metric given by (18).

VII. ANALYTIC CALCULATION OF DIFFUSIVE MODES IN MASSIVE-GRAVITY MODEL

In this section, we will show that the QNMs of charged scalar field perturbation in the spacetime with nonzero Λ and γ are purely imaginary for $\ell = 0$. This is the result of the boundary conditions on the scalar field at the far region $r \gg 1$.

A. AdS case

First, we will consider asymptotically AdS space with $\Lambda = -3/L^2$. Start with the equation of motion (22) in the far region of the radial part $R(r) = \phi(r)/r$,

$$\left(\gamma r + \frac{r^2}{L^2}\right)R''(r) + \left(3\gamma + \frac{4r}{L^2}\right)R'(r) + \left[\frac{\omega^2}{(\gamma r + \frac{r^2}{L^2})} - \left(\frac{\ell(\ell+1)}{r^2} + m_s^2\right)\right]R(r) = 0, \quad (67)$$

where we have approximated $f(r) \simeq \gamma r + r^2/L^2$ in the far region. In a new coordinate,

$$y \equiv 1 + \frac{r}{\gamma L^2}, \quad (68)$$

the equation of motion in the far region can be rewritten as

$$y(1-y)\frac{d^2R}{dy^2} + (1-4y)\frac{dR}{dy} + \left[\frac{\omega^2/\gamma^2}{y(1-y)} + \left(\frac{\ell(\ell+1)}{\gamma^2 L^2 (1-y)^2} + m_s^2 L^2\right)\right]. \quad (69)$$

To simplify the calculation, we set $\ell = 0$; the equation then has the solution

$$R(y) = y^{-i\bar{\omega}}(1-y)^{-1+\sqrt{1-\bar{\omega}^2}}h(y), \quad (70)$$

where

$$h(y) = A\,{}_2F_1(a,b,c;y) + B(-y)^{2i\bar{\omega}}\,{}_2F_1(\bar{\omega} \to -\bar{\omega}), \quad (71)$$

when ${}_2F_1(a,b,c;y)$ is the hypergeometric function with

$$a = -i\bar{\omega} + \frac{1}{2} + \sqrt{1-\bar{\omega}^2} - \frac{1}{2}\sqrt{9+4m^2}, \quad (72)$$

$$b = -i\bar{\omega} + \frac{1}{2} + \sqrt{1-\bar{\omega}^2} + \frac{1}{2}\sqrt{9+4m^2}, \quad (73)$$

and $c = 1 - 2i\bar{\omega}$. We have used dimensionless parameters $\bar{\omega} \equiv \omega/\gamma, m \equiv m_s L$. A and B are constants to be determined by the boundary conditions. Note that the second term on the rhs of (71) is exactly the symmetric $\bar{\omega} \to -\bar{\omega}$ of the first term. For consideration of the QNMs, it suffices to consider only the first term of the solution.

In the far region $r \gg 1$, we can use Euler's transformation on the hypergeometric function to obtain

$$R(y) \sim \left(\frac{r}{\gamma L^2}\right)^{-\frac{3}{2}+\frac{3}{2}\sqrt{1+4m^2/9}} \frac{\Gamma(c)\Gamma(b-a)}{\Gamma(b)\Gamma(c-a)}, \quad (74)$$

where we have used the identity

$${}_2F_1(a,c-b,c;1) = \frac{\Gamma(c)\Gamma(b-a)}{\Gamma(c-a)\Gamma(b)}.$$

For $m^2 < 0$, the exponent of $r/\gamma L^2$ in (74) is negative, the solution is vanishing at infinity, and there is no requirement on the $\bar{\omega}$. For $m^2 \geq 0$, on the other hand, the exponent is positive, and we need the poles of the Gamma function to suppress the solution at infinity, i.e.,

$$-i\bar{\omega} + \frac{1}{2} \pm \sqrt{1-\bar{\omega}^2} + \sqrt{9+4m^2} = -N, \quad (75)$$

where N is a non-negative integer. This leads to the QNMs

$$\omega = -i\gamma\frac{(N + \frac{1}{2}(1+\sqrt{9+4m^2}))^2 - 1}{2(N + \frac{1}{2}(1+\sqrt{9+4m^2}))}, \quad (76)$$

for $N = 0, 1, 2, \ldots$. However, the QNMs also need to satisfy the boundary condition at small r. By using Pfaff's transformation

$$ {}_2F_1(a,b,c;z) = (1-z)^{c-a-b}\,{}_2F_1(c-a,c-b,c;z), \tag{77}$$

the far-region solution for small r can be expressed as

$$\begin{aligned} R(y) &\sim \left(\frac{r}{\gamma L^2}\right)^{-1+\sqrt{1-\bar{\omega}^2}} \left(1+\frac{r}{\gamma L^2}\right)^{-i\bar{\omega}} \\ &\quad \times \left(\frac{-r}{\gamma L^2}\right)^{c-b-a} {}_2F_1(c-a,c-b,c;y), \\ &\sim \left(\frac{r}{\gamma L^2}\right)^{-1-\sqrt{1-\bar{\omega}^2}} \frac{\Gamma(c)\Gamma(2\sqrt{1-\bar{\omega}^2})}{\Gamma(a)\Gamma(b)}. \end{aligned} \tag{78}$$

For the solution to be vanishing, it is required that $b = -N$ [$a = -N$ is not consistent with (76)], giving again the condition (76). There is a distinct difference between an asymptotically AdS space with and without the massive-gravity effect γ. The QNMs we found here are diffusive in nature with pure imaginary values that exist only when γ is nonzero. Numerical analysis confirms these diffusive modes as shown in Fig. 4. The existence of a small black hole in the small-r region changes the values of these diffusive QNMs by a small quantity, however, in addition to generating other possible vibrating modes of the QNMs. These other possible modes already exist in a small AdS black hole in conventional Einstein gravity.

B. dS case

A similar calculation can be performed in the asymptotically dS case with $\Lambda > 0$. The equation of motion in the new coordinate $y \equiv 1 - r/\gamma L^2$ can be written as

$$\begin{aligned} &y(1-y)\frac{d^2R}{dy^2} + (1-4y)\frac{dR}{dy} \\ &\quad + \left[\frac{\omega^2/\gamma^2}{y(1-y)} + \left(\frac{\ell(\ell+1)}{\gamma^2L^2(1-y)^2} - m_s^2L^2\right)\right]. \end{aligned} \tag{79}$$

This is $L^2 \to -L^2$ of (69), so it has exactly the same solution as (70) and (71) with $m^2 \to -m^2$. Certainly, the far region is different since the spacetime boundary now becomes the cosmic horizon at $r_c = \gamma L^2$. Similar to the AdS case, the far-region solution for $\ell = 0$ in the small-r limit ($y \to 1$) takes the forms

$$\begin{aligned} R(y) &\sim \left(\frac{r}{\gamma L^2}\right)^{-1-\sqrt{1-\bar{\omega}^2}} {}_2F_1(c-a',c-b',c;1), \\ &\sim \left(\frac{r}{\gamma L^2}\right)^{-1-\sqrt{1-\bar{\omega}^2}} \frac{\Gamma(c)\Gamma(2\sqrt{1-\bar{\omega}^2})}{\Gamma(a')\Gamma(b')}, \end{aligned} \tag{80}$$

where $a' = a(m^2 \to -m^2)$ and $b' = b(m^2 \to -m^2)$, respectively. Therefore, we have the QNMs given by

$$\omega = -i\gamma \frac{(N+\frac{1}{2}(1+\sqrt{9-4m^2}))^2 - 1}{2(N+\frac{1}{2}(1+\sqrt{9-4m^2}))}, \tag{81}$$

for $N = 0, 1, 2, \ldots$ in order to make the far-region solution vanish at small r.

The QNMs considered will certainly be modified by the presence of a black hole, either by developing real parts and new QNMs or shifting the imaginary values of the original diffusive modes unique to the massive-gravity model. As is argued in Ref. [22], turning on the electric potential at the horizon should simply shift the real parts of QNMs by $qA_h = qQ/r_h$ for the asymptotically AdS case. In the dS case, the results in Tables I–III show that shifts of the real parts of QNMs in the near-horizon regions are actually $qQ/2r_h(qQ/2r_c)$ for the near-$r_h(r_c)$ solutions. In the presence of massive-gravity parameter γ, shifts in the real parts also depend on γ as shown in Table I.

VIII. CONCLUSIONS

In this paper, we have studied the effect of massive charged scalar perturbations on charged black hole spacetime in dRGT massive gravity. Notable effects of massive gravity are the generation of the cosmological constant term and the linear term in the metric (18) from the combination of massive graviton mass, cubic and quartic graviton interactions, and the fiducial metric. Physically, only the fiducial metric determines the linear γr term in the sense that it will be zero if c is vanishing. A physical interpretation of the fiducial metric is an extra-dimensional pullback from the bulk metric [45] or from the second site of the two-site theory [46]. We have explored the effect of the γ term on the spacetime structure. It is found that the spacetime structure is very sensitive to the value of γ. For the dS case, the metric (18) has three positive real roots associated with the Cauchy horizon, the event horizon, and the cosmological horizon, respectively. At some fixed value of γ, we obtain an extremal charged black hole where the Cauchy and event horizon of black hole coincide. For the AdS case, one can have a standard charged AdS black hole, an extremal charged AdS black hole, or even regular spacetime with no horizon depending on the value of γ.

In Sec. V, the QNMs of a black hole in asymptotically dS space in the dRGT model are computed. The numerical scheme called the asymptotic iteration method [33] is applied for calculating the quasinormal frequencies. We find unstable modes for the lowest angular harmonic index $\ell = 0$. Some of these unstable modes live in the superradiant regime. However, not all the superradiant modes are unstable. On the other hand, we find no evidence of any instabilities for $\ell = 2$. All the dS black holes we investigate in this case appear to be stable under small perturbation. Since the perturbation decays with time, these scalar modes do not suffer from the superradiant instability. The QNMs for the all-region solutions are also computed via the

third-order WKB approximation and are in good agreement with the results obtained from the AIM. With $q = 0$, the quasinormal frequencies with a vanishing real part (the diffusive mode) are discovered. We find that as q increases the real part of ω is shifted up by $qQ/2r_h(qQ/2r_c)$ for these modes. They correspond to the near-event (cosmic)-horizon solutions. In addition, when q is nonzero, the normal mode with zero imaginary parts is found as the lowest possible mode. Finally, it is found that the black holes become more stable as γ gets larger.

In Sec. VI, the QNMs of a black hole in asymptotically AdS space in dRGT massive gravity are explored. For a small black hole in negative cosmological constant spacetime, the QNMs have asymptotic linear dependence on the mode number n. This can be shown using the monodromy method and other approximation schemes (see, e.g., Ref. [31] and references therein) for asymptotically AdS space in conventional Einstein gravity. In the massive-gravity model considered here, the linearity persists as long as the massive-gravity effect does not regulate or alternate the black hole spacetime. Charged perturbation of the scalar field in the charged AdS black hole background could become unstable with positive imaginary parts of QNMs (Fig. 5). Massive-gravity effects reduce the energy of these unstable modes but leave the characteristic time almost unchanged. In a holographic viewpoint, the gauge theory dual of these situations is possibly the condensation of charged scalar (quasi)particles resulting in a superconducting phase.

Analytic calculation of the QNMs in the spacetime with massive-gravity parameter γ in Sec. VII shows that the QNMs form a diffusive tower with the size proportional to γ for $\ell = 0$. In contrast to empty AdS in which all the QNMs are normal modes, the linear term γr in the metric induces a pseudohorizon at $r = 0$ in the asymptotically far region, rendering all QNMs imaginary. Numerical results in both dS and AdS cases confirm the existence of these modes, albeit deformed by the presence of a black hole in the background.

As a possible extension of this work, a time-domain analysis of linear charged scalar perturbation on charged dRGT black hole background is needed to confirm the frequency-domain stability presented in this paper. Since we have shown that the AdS black holes are superradiantly unstable, therefore, it would be an interesting task to investigate the end point of this instability. Many works have suggested that a hairy black hole could be the end point of superradiant instability [47–49]. A possible end point of a black hole in the dRGT model could be a black hole with massive graviton hair similar to the one studied in Ref. [50].

ACKNOWLEDGMENTS

We would like to thank Napat Poovuttikul for useful discussions. L. T. is supported by the National Research Foundation of Korea (NRF) grant funded by the Korea government (MSIP) (Grant No. 2016R1C1B1010107). S. P. is supported by the Theoretical and Computational Science (TaCS) Center under Computational and Applied Science for Smart Innovation Cluster, Faculty of Science, KMUTT.

APPENDIX: WKB APPROXIMATION

To study QNMs of black holes, since the equation of linear perturbation of a black hole can be recast into the Schrödinger-like form, one may apply WKB approximation to estimate possible modes of a black hole. In conventional quantum mechanics, the essence of the WKB method involves considering approximate solutions to each asymptotic region and matching them together to obtain approximated QNMs of the black hole. The WKB approach makes use of a Schrödinger-like differential equation of the following form [51–54]:

$$\frac{d^2\phi}{dr_*^2} + \mathcal{Q}(r_*)\phi = 0. \tag{A1}$$

Comparing this with (23), we can find the corresponding $\mathcal{Q}$:

$$\mathcal{Q} = (\omega + qA_0)^2 - f\left(m_s^2 + \frac{\ell(\ell+1)}{r^2} + \frac{f'}{r}\right). \tag{A2}$$

In the Schrödinger equation language, $\mathcal{Q}$ is equivalent to $2m(E-U)/\hbar^2$, where m is the mass, E is the energy, and U is the potential of a one-dimensional system. Despite the probably complex form of $\mathcal{Q}$, the property of $\mathcal{Q}$ around its extremum r_{*0} can be approximated to be that of a parabola. To this end, we can perform a Taylor expansion of $\mathcal{Q}$ around its extremum point as

$$\mathcal{Q}(r_*) = \mathcal{Q}(r_{*0}) + \frac{1}{2}\mathcal{Q}''(r_{*0})(r_* - r_{*0})^2 + \cdots,$$
$$\mathcal{Q}'(r_{*0}) = 0, \tag{A3}$$

where a prime denotes a derivative with respect to r_*. From now on, we will use the following shorthand notation:

$$\mathcal{Q}_0 \equiv \mathcal{Q}(r_{*0}), \qquad \mathcal{Q}_0'' \equiv \mathcal{Q}''(r_{*0}), \quad \text{and so on.} \tag{A4}$$

Through this expansion, it is clear that we can estimate a solution around r_{*0} to be that of a system of which $\mathcal{Q}$ (or the corresponding potential U) is a parabola. By requiring the boundary condition for QNMs (the near-horizon field goes into the black hole, and the field at $r \to \infty$ goes outward to ∞), it is possible to obtain the matching condition from the approximate solution,

$$\frac{i\mathcal{Q}_0}{\sqrt{2\mathcal{Q}_0''}} - i\bar{\Lambda} - \Omega = \left(n + \frac{1}{2}\right), \tag{A5}$$

where

$$\bar{\Lambda} = \frac{1}{(2\mathcal{Q}_0'')^{1/2}}\left[\frac{1}{8}\left(\frac{\mathcal{Q}_0^{(4)}}{\mathcal{Q}_0''}\right)\left(\frac{1}{4}+\alpha^2\right) - \frac{1}{288}\left(\frac{\mathcal{Q}_0'''}{\mathcal{Q}_0''}\right)^2(7+60\alpha^2)\right], \tag{A6}$$

$$\Omega = \frac{\alpha}{2\mathcal{Q}_0''}\left[\frac{5}{6912}\left(\frac{\mathcal{Q}_0'''}{\mathcal{Q}_0''}\right)^4(77+188\alpha^2) - \frac{1}{384}\left(\frac{\mathcal{Q}_0'''^2\mathcal{Q}_0^{(4)}}{\mathcal{Q}_0''^3}\right)(51+100\alpha^2) + \frac{1}{2304}\left(\frac{\mathcal{Q}_0^{(4)}}{\mathcal{Q}_0''}\right)^2(67+68\alpha^2) - \frac{1}{288}\left(\frac{\mathcal{Q}_0'''\mathcal{Q}_0^{(5)}}{\mathcal{Q}_0''^2}\right)(19+28\alpha^2) - \frac{1}{288}\left(\frac{\mathcal{Q}_0^{(6)}}{\mathcal{Q}_0''}\right)(5+4\alpha^2)\right], \tag{A7}$$

$$\alpha \equiv n+\frac{1}{2}, \quad n \in \{0,1,2,\ldots\} \quad \text{for } \mathrm{Re}(\omega) > 0. \tag{A8}$$

$$\alpha \equiv n+\frac{1}{2}, \quad n \in \{0,1,2,\ldots\} \quad \text{for } \mathrm{Re}(\omega) > 0. \tag{A9}$$

The fundamental mode is represented by $n = 0$. Particularly, the first term on the left-hand side of (A5) corresponds to the first-order WKB approximation [51], and the second term and the third term correspond to the second-order and third-order WKB approximations, respectively [52,53].

In the Schwarzschild case, $\mathcal{Q}$ can be expressed as $\mathcal{Q} = \omega^2 - V(r_*)$, and V is an ω-independent function, which simply makes the evaluation of the second derivative of $\mathcal{Q}$ relatively easy. However, in general, each order of the derivative of $\mathcal{Q}$ depends on ω, which makes the matching condition cumbersome to deal with. In our study, we use the following techniques. First, we rewrite (A5) as follows:

$$i\mathcal{Q}_0 = \sqrt{2\mathcal{Q}_0''}\left(i\bar{\Lambda}+\Omega+\left(n+\frac{1}{2}\right)\right). \tag{A10}$$

We then substitute $\mathcal{Q}_0$ by using (A2) as follows:

$$\left[(\omega+qA_0)^2 - f\left(m_s^2+\frac{\ell(\ell+1)}{r^2}+\frac{f'}{r}\right)\right]\Big|_{r_0} = \frac{\sqrt{2\mathcal{Q}_0''}}{i}\left(i\bar{\Lambda}+\Omega+\left(n+\frac{1}{2}\right)\right). \tag{A11}$$

To approximate the quasinormal frequencies, we will perform an iteration using (A11). Given a random value of ω_0, we compute for $r_0(\omega_0)$, which minimizes $\mathcal{Q}(\omega_0)$; then, we find ω_1 from the following:

$$(\omega_1+qA_0(r_0))^2 - \left[f\left(m_s^2+\frac{\ell(\ell+1)}{r^2}+\frac{f'}{r}\right)\right]\Big|_{r_0} = \frac{\sqrt{2\mathcal{Q}_0''(r_0,\omega_0)}}{i}\left(i\bar{\Lambda}(r_0,\omega_0)+\Omega(r_0,\omega_0)+\left(n+\frac{1}{2}\right)\right). \tag{A12}$$

Furthermore, we find successive ω_i iteratively via a similar equation,

$$(\omega_{i+1}+qA_0(r_0))^2 - \left[f\left(m_s^2+\frac{\ell(\ell+1)}{r^2}+\frac{f'}{r}\right)\right]\Big|_{r_0} = \frac{\sqrt{2\mathcal{Q}_0''(r_0,\omega_i)}}{i}\left(i\bar{\Lambda}(r_0,\omega_i)+\Omega(r_0,\omega_i)+\left(n+\frac{1}{2}\right)\right), \tag{A13}$$

where $r_0 = r_0(\omega_i)$ in this case. The iteration is performed until the difference between successive frequencies is less than 1%, and we take the frequency from the last iteration to be our approximate quasinormal frequency.

In spite of the simple procedures, the WKB approximation is said to yield satisfactory results when the azimuthal number ℓ is greater than n. Moreover, since we consider two kinds of black hole solutions, dS and AdS black holes, the matching condition used here only corresponds to the dS case. In the dS case, the field at $r \to \infty$ tends to propagate outward as a plane wave, while this is not the case in the AdS case. The matching techniques in Refs. [51–53] only utilize the boundary condition of a field propagating outward and thus correspond to the property of the far-field limit in dS geometry.

[1] V. Bonvin *et al.*, H0LiCOW V. New COSMOGRAIL time delays of HE 04351223: H_0 to 3.8 percent precision from strong lensing in a flat CDM model, Mon. Not. R. Astron. Soc. **465**, 4914 (2017).

[2] B. P. Abbott *et al.* (LIGO Scientific and Virgo Collaborations), Tests of General Relativity with GW150914, Phys. Rev. Lett. **116**, 221101 (2016).

[3] C. de Rham, J. T. Deskins, A. J. Tolley, and S. Y. Zhou, Graviton mass bounds, Rev. Mod. Phys. **89**, 025004 (2017).

[4] M. Fierz and W. Pauli, On relativistic wave equations for particles of arbitrary spin in an electromagnetic field, Proc. R. Soc. A **173**, 211 (1939).

[5] H. van Dam and M. J. G. Veltman, Massive and massless Yang-Mills and gravitational fields, Nucl. Phys. **B22**, 397 (1970).

[6] V. I. Zakharov, Linearized gravitation theory, and the graviton mass, Pis'ma Zh. Eksp. Teor. Fiz. **12**, 447 (1970) [JETP Lett. **12**, 312 (1970)].

[7] A. I. Vainshtein, To the problem of nonvanishing gravitation mass, Phys. Lett. **39B**, 393 (1972).

[8] C. de Rham, A. J. Tolley, and S. Y. Zhou, The Λ_2 limit of massive gravity, J. High Energy Phys. 04 (2016) 188.

[9] D. G. Boulware and S. Deser, Can gravitation have a finite range?, Phys. Rev. D **6**, 3368 (1972).

[10] C. de Rham and G. Gabadadze, Generalization of the Fierz-Pauli action, Phys. Rev. D **82**, 044020 (2010).

[11] C. de Rham, G. Gabadadze, and A. J. Tolley, Resummation of Massive Gravity, Phys. Rev. Lett. **106**, 231101 (2011).

[12] G. D'Amico, C. de Rham, S. Dubovsky, G. Gabadadze, D. Pirtskhalava, and A. J. Tolley, Massive cosmologies, Phys. Rev. D **84**, 124046 (2011).

[13] A. E. Gumrukcuoglu, C. Lin, and S. Mukohyama, Open FRW universes and self-acceleration from nonlinear massive gravity, J. Cosmol. Astropart. Phys. 11 (2011) 030.

[14] A. E. Gumrukcuoglu, C. Lin, and S. Mukohyama, Cosmological perturbations of self-accelerating universe in nonlinear massive gravity, J. Cosmol. Astropart. Phys. 03 (2012) 006.

[15] R. G. Cai, Y. P. Hu, Q. Y. Pan, and Y. L. Zhang, Thermodynamics of black holes in massive gravity, Phys. Rev. D **91**, 024032 (2015).

[16] S. G. Ghosh, L. Tannukij, and P. Wongjun, A class of black holes in dRGT massive gravity and their thermodynamical properties, Eur. Phys. J. C **76**, 119 (2016).

[17] A. De Felice and S. Mukohyama, Towards consistent extension of quasidilaton massive gravity, Phys. Lett. B **728**, 622 (2013).

[18] A. De Felice, A. E. Gumrukcuoglu, and S. Mukohyama, Generalized quasi-dilaton theory, Phys. Rev. D **88**, 124006 (2013).

[19] J. D. Bekenstein, Extraction of energy, and charge from a black hole, Phys. Rev. D **7**, 949 (1973).

[20] J. C. Degollado, C. A. R. Herdeiro, and H. F. Runarsson, Rapid growth of superradiant instabilities for charged black holes in a cavity, Phys. Rev. D **88**, 063003 (2013).

[21] J. C. Degollado and C. A. R. Herdeiro, Time evolution of superradiant instabilities for charged black holes in a cavity, Phys. Rev. D **89**, 063005 (2014).

[22] N. Uchikata and S. Yoshida, Quasinormal modes of a massless charged scalar field on a small Reissner-Nordstrom-anti-de Sitter black hole, Phys. Rev. D **83**, 064020 (2011).

[23] Z. Zhu, S. J. Zhang, C. E. Pellicer, B. Wang, and E. Abdalla, Stability of Reissner-Nordstrom black hole in de Sitter background under charged scalar perturbation, Phys. Rev. D **90**, 044042 (2014); Publisher's Note, Phys. Rev. D **90**, 049904 (2014).

[24] R. A. Konoplya and A. Zhidenko, Charged scalar field instability between the event and cosmological horizons, Phys. Rev. D **90**, 064048 (2014).

[25] V. Cardoso, O. J. C. Dias, J. P. S. Lemos, and S. Yoshida, The black hole bomb and superradiant instabilities, Phys. Rev. D **70**, 044039 (2004); Publisher's Note, Phys. Rev. D **70**, 049903 (2004).

[26] V. Cardoso and O. J. C. Dias, Small Kerr-anti-de Sitter black holes are unstable, Phys. Rev. D **70**, 084011 (2004).

[27] V. Cardoso, J. C. Dias, G. S. Hartnett, L. Lehner, and J. E. Santos, Holographic thermalization, quasinormal modes and superradiance in Kerr-AdS, J. High Energy Phys. 04 (2014) 183.

[28] R. Brito, V. Cardoso, and P. Pani, Superradiance: Energy extraction, black-hole bombs and implications for astrophysics and particle physics, Lect. Notes Phys. **906**, 1 (2015).

[29] P. Prasia and V. C. Kuriakose, Quasi normal modes and P-V criticallity for scalar perturbations in a class of dRGT massive gravity around black holes, Gen. Relativ. Gravit. **48**, 89 (2016).

[30] There is a possibility thatϵ is extremely small but not zero; its size is constrained by the flatness of empty space in the spacetime; for simplicity we will simply assume $\epsilon = 0$ here.

[31] E. Berti, V. Cardoso, and A. O. Starinets, Quasinormal modes of black holes and black branes, Classical Quantum Gravity **26**, 163001 (2009).

[32] A. Zhidenko, Quasinormal modes of Schwarzschild de Sitter black holes, Classical Quantum Gravity **21**, 273 (2004).

[33] H. Ciftci, R. L. Hall, and N. Saad, Asymptotic iteration method for eigenvalue problems, J. Phys. A **36**, 11807 (2003).

[34] H. T. Cho, A. S. Cornell, J. Doukas, and W. Naylor, Black hole quasinormal modes using the asymptotic iteration method, Classical Quantum Gravity **27**, 155004 (2010).

[35] M. Kord Zangeneh, B. Wang, A. Sheykhi, and Z. Y. Tang, Charged scalar quasi-normal modes for linearly charged dilaton-Lifshitz solutions, Phys. Lett. B **771**, 257 (2017).

[36] I. G. Moss and J. P. Norman, Gravitational quasinormal modes for anti-de Sitter black holes, Classical Quantum Gravity **19**, 2323 (2002).

[37] W. Naylor, https://wadenaylorphysics.wordpress.com/aim/.

[38] We will not compare the results from the AIM and WKB for the data in Table I. This is because the accuracy of the third-order WKB approximation is good for $\ell > n$, where n is a fundamental mode. In addition, for a given n, the accuracy of the WKB method increases with ℓ.

[39] Sample codes can be found at http://msstp.org/?q=node/289.

[40] I. Arav and Y. Oz, The sound of topology in the AdS/CFT correspondence, J. High Energy Phys. 12 (2012) 014.
[41] M. Wang and C. Herdeiro, Superradiant instabilities in a D-dimensional small Reissner-Nordstrom-anti-de Sitter black hole, Phys. Rev. D **89**, 084062 (2014).
[42] S. S. Gubser, Breaking an Abelian gauge symmetry near a black hole horizon, Phys. Rev. D **78**, 065034 (2008).
[43] G. T. Horowitz and V. E. Hubeny, Quasinormal modes of AdS black holes and the approach to thermal equilibrium, Phys. Rev. D **62**, 024027 (2000).
[44] V. Cardoso, R. Konoplya, and J. P. S. Lemos, Quasinormal frequencies of Schwarzschild black holes in anti-de Sitter spacetimes: A complete study of the overtone asymptotic behavior, Phys. Rev. D **68**, 044024 (2003).
[45] G. Gabadadze and S. Yu, Metamorphosis of the cosmological constant and 5D origin of the fiducial metric, Phys. Rev. D **94**, 104059 (2016).
[46] N. Arkani-Hamed, H. Georgi, and M. D. Schwartz, Effective field theory for massive gravitons and gravity in theory space, Ann. Phys. (Amsterdam) **305**, 96 (2003).
[47] S. R. Dolan, S. Ponglertsakul, and E. Winstanley, Stability of black holes in Einstein-charged scalar field theory in a cavity, Phys. Rev. D **92**, 124047 (2015).
[48] N. Sanchis-Gual, J. C. Degollado, C. Herdeiro, J. A. Font, and P. J. Montero, Dynamical formation of a Reissner-Nordstrom black hole with scalar hair in a cavity, Phys. Rev. D **94**, 044061 (2016).
[49] P. Bosch, S. R. Green, and L. Lehner, Nonlinear Evolution and Final Fate of Charged Anti-de Sitter Black Hole Superradiant Instability, Phys. Rev. Lett. **116**, 141102 (2016).
[50] R. Brito, V. Cardoso, and P. Pani, Black holes with massive graviton hair, Phys. Rev. D **88**, 064006 (2013).
[51] B. F. Schutz and C. M. Will, Black hole normal modes: a semianalytic approach, Astrophys. J. **291**, L33 (1985).
[52] S. Iyer and C. M. Will, Black hole normal modes: A WKB approach. 1. Foundations and application of a higher order WKB analysis of potential barrier scattering, Phys. Rev. D **35**, 3621 (1987).
[53] R. A. Konoplya, Quasinormal behavior of the d-dimensional Schwarzschild black hole, and higher order WKB approach, Phys. Rev. D **68**, 024018 (2003).
[54] R. A. Konoplya and A. Zhidenko, Quasinormal modes of black holes: From astrophysics to string theory, Rev. Mod. Phys. **83**, 793 (2011).